Electronic Supplementary Information

Electrocatalytic water oxidation with a tris-chelating bipyridine/bis-pyrimidinethiolate Co(III) complex covalently immobilized onto MoS_2 nanosheets

Michail P. Minadakis,[a] Dimitra K. Gioftsidou,[b] Panagiotis A. Angaridis,[b] Verónica Pérez Luna,[c] Mildred Quintana,[c] Ruben Canton-Vitoria,[d,e] and Nikos Tagmatarchis*[a]

[a] Theoretical and Physical Chemistry Institute, National Hellenic Research Foundation, 48 Vassileos Constantinou Avenue, Athens 11635, Greece. Email: tagmatar@eie.gr

[b] Laboratory of Inorganic Chemistry, Department of Chemistry, Aristotle University of Thessaloniki, Thessaloniki 54124, Greece.

[c] High Resolution Microscopy-CICSaB and Faculty of Science, Universidad Autonóma de San Luis Potosi, Av. Sierra Leona 550, Lomas de San Luis Potosi, 78210 SLP, Mexico.

[d] Department of Materials Chemistry & Institute of Materials and Systems for Sustainability (IMaSS), Nagoya University, Nagoya 464-8601, Japan.

[e] Joining and Welding Research Institute, The University of Osaka, Osaka 567-0047, Japan.

Materials

All chemicals and solvents were commercially available and used as received unless otherwise stated. All solvents as well as chlorosulfonic acid (HSO_3Cl) were purchased from Honeywell (Diegem, Belgium) and were of analytical grade. Molybdenum disulfide powder (particle size ~6 μm) was purchased from Sigma Aldrich (Merck KGaA group, Darmstadt, Germany). Isoamyl (isopentyl) nitrite (with 0.2% anhydrous sodium carbonate as stabilizer) was purchased from Fluorochem (Cork, Ireland). Nafion 5% alcohol solution (DE520 CS type) was purchased from Fujifilm (Ratingen, Germany). PTFE filters (47 mm diameter, 0.2 μm pore size) were purchased from ADVANTEC, Japan. For the synthesis of the Co(III) complex, all manipulations were carried out under atmospheric conditions. $CoCl_2{\cdot}6H_2O$, 2-pyrimidinethiol (pymtH), 1,10-phenanthroline (phen), ammonium hexafluorophosphate (NH_4PF_6) and sodium methoxide (CH_3ONa) were purchased from commercial sources and used as received.

Instrumentation

Probe sonication was performed with a Bandelin Sonopuls Ultrasonic Homogenizer HD 3200 equipped with a flat head probe (VS-70T), running at 40% amplitude (100 W) of the maximum power (250 W) with the pulse set for 5 s ON/5 s OFF.

Mid-infrared spectra in 525-4000 cm^{-1} region were acquired on a Fourier transform IR spectrometer (Tensor II, Bruker Optics) equipped with a single reflection diamond ATR accessory (DuraSamp1IR II, SensIR Technologies). Typically, 100 scans were acquired at 4 cm^{-1} resolution.

Micro-Raman scattering measurements were performed at room temperature (25 ± 2 °C) in the backscattering geometry using a RENISHAW inVia Raman spectrometer equipped with a CCD camera and a Leica microscope. A 1200 lines mm^{-1} grating was used for all measurements, providing a spectral resolution of ± 1 cm^{-1}. As the excitation source, a He/Ne laser line of 633 nm was used. Acquisitions were collected at the 100-2000 cm^{-1} region on extended mode, with 10 s of exposure time and laser power 50% (corresponding to ~0.3 mW cm^{-2}) to avoid overheating of the samples. The laser spot was focused on the sample surface using a long working distance 50x objective lens. Raman spectra were collected after map image acquisition was conducted on different areas of the sample and recorded with Peltier cooled CCD camera. The intensity ratio A_{1g}/2LA(M) was obtained by dividing the peak intensities, following any baseline corrections. For the Raman spectral maps, 3 different areas of 121 acquisition points were scanned for every sample, and the most representative as well as closest to the average of sole acquisitions is outlined. The data were processed with Renishaw Wire V4.3 and Origin Pro 8 software.

UV-Vis absorption spectra were recorded on a PerkinElmer (Lambda 19) UV-Vis-NIR spectrophotometer (200-2500 nm) with PMT detector (deuterium lamp as the light source for UV, halogen lamp for Vis/NIR), at a scan speed of 480 nm min^{-1}, 2 nm slit width and 1 nm interval for data acquisition.

Transmission electron microscopy (TEM) images were acquired using a JEM-JEOL 2100 microscope operated at 200 kV. The sample was prepared by dispersing it in isopropanol and drop-casting onto a lacey carbon grid (Lacey carbon, 300 mesh, carbon). Elemental analysis was carried out with an EDAX X-ray detector.

Thermogravimetric analysis (TGA) was performed on a TGA Q500 V20.2 Build 27 instrument (TA, Eschborn, Germany) under N5.0 (99.999%) purity grade N_2 atmosphere and standard balance (40 mL min^{-1}) and sample (60 mL min^{-1}) flows. In a typical experiment, 1-2 mg of the nanomaterial under analysis were placed in a Pt pan (prior to the experiment, any impurities on the Pt pan were burned off using a commercial blowtorch). Subsequently, the material was subjected to the following experimental procedure: temperature equilibration at 100 °C, isotherm at 100 °C for 10 min., and ramp up to 800 °C at a rate of 10 °C min^{-1}. Mass changes were recorded as a function of temperature. Differential thermograph (DTG) was also recorded to aid with the determination of the decomposition profile of each compound. The results were analyzed with Instrumental analysis V5.5.23 and Origin Pro 8 software.

Electrochemical analysis

All electrochemical OER measurements were carried out on an Autolab PGSTAT128N (Metrohm, Herisau, Switzerland) potentiostat-galvanostat in a standard three-compartment electrochemical cell using a ring-disk electrode (RDE) with glassy carbon (GC) surface (3 mm diameter) as the working electrode (WE). A freshly prepared aqueous 0.1 M KOH solution (pH = 13) was used as the electrolyte and was purged for 30 min. prior to the experiments and throughout the ORR measurements with N_2 to achieve saturation. A platinum foil was used as the counter electrode (CE) and a mercury oxide electrode (MOE, Hg/HgO) with aqueous 0.1 M KOH as the filling solution, was applied as the reference electrode (RE). The catalyst inks was prepared by dispersing 1.0 mg of the catalyst powder in a 250 μL mixture of distilled water, isopropanol, and 5% Nafion alcohol solution (v/v/v = 4:1:0.02) and sonicated for 30 min. prior to use. Before drop casting the electrocatalytic ink on the electrode surface, the working electrode was polished with fine Al_2O_3 powder and thoroughly rinsed with distilled water. Afterwards, a 3 μL aliquot (0.012 mg & 169 μg cm^{-2} catalyst loading) of the electrocatalytic ink was drop-casted on the electrode surface and was dried under N_2 stream to furnish a thin coating film (TF-RDE).

Linear sweep voltammograms (LSV) were collected (1600 RPM, 5 mV s^{-1} scan rate) in N_2 saturated electrolyte at ambient temperature (24 ± 2 °C) for each different catalyst. Recorded current was normalized and presented as current density via RDE geometric surface area ($\mathbf{A_{geom}}$=0.071 cm^2).

Tafel slopes were extracted by plotting overpotential ($\boldsymbol{\eta}$ = E-E^0, where E^0=1.23 V vs RHE) versus logarithm of normalized current density [$\mathbf{log(j_{geom})}$] and presented as mV dec^{-1}.

Electrochemical impedance spectroscopy (EIS) was conducted from 10^5 to 10^{-1} Hz with an AC amplitude of 0.01 V.

Electrochemically active surface area (**ECSA**) was calculated via graphically extracted double layer capacitance ($\mathbf{C_{dl}}$) and specific capacitance of a flat electrode ($\mathbf{C_s}$) for which the value used was 40 μF cm^{-2}. We assumed this specific value since it is considered the average value for electrode materials (C, Ni, Co, etc.) and it is the experimental standard in literature. Cyclic voltammograms were recorded in different scan rates (50-500 mV s^{-1}) in a non-Faradaic 200 mV window and the values of $j_{anode}/j_{cathode}$ were taken at the center of each CV (1.4 V vs RHE). By dividing the $\mathbf{C_{dl}}$ value with $\mathbf{C_s}$ value, roughness factor (**RF**) is obtained. Multiplication of RF with geometric surface area ($\mathbf{A_{geom}}$=0.071 cm^2) yields ECSA.

XPS: An ultrathin film of the material was formed on the surface of water by carefully contacting a few drops of a 1 mg/mL dispersion of the material in MeOH. The film was subsequently collected using a silicon wafer coated with 50 nm of gold, previously treated for 15 min with piranha solution. The films were dried for 15 min at 100 °C in air. Subsequently, a PHI Versa Probe III instrument was utilized to record the spectrum. The pressure of the system was smaller than $1x10^{-7}$ Torr. For excitation, a monochromatic aluminum X-ray source (Al Kα) with an energy of 1486.6 eV was used and an Ar ion beam was employed for charge removal.

Synthetic Procedures

5-nitro-1,10-phenanthroline (5-NO_2-phen). 2.000 g of 1,10-phenanthroline (11.1 mmol) was dissolved in 12 mL of ice cold concentrated H_2SO_4 solution and then 6 mL of concentrated HNO_3 were slowly added dropwise. The reaction mixture was stirred for 3 h at 160 °C and then poured into crushed ice. Saturated aqueous NaOH solution (25 mL) was added to the reaction solution to adjust the pH at ~ 3. **5-NO_2-phen** precipitated as a yellow solid, filtered off, washed with H_2O (40 mL) and dried under vacuum for 4 h. Yield: 1.96 g (98 %). Anal. Calcd (%) for $C_{12}H_7N_3O_2$: C, 64.00; H, 3.13; N, 18.66. Found (%): C, 63.02; H, 3.23; N, 17.52. ^1H NMR (500 MHz, $CDCl_3$): δ (ppm) 9.36 (s, 1 H), 9.31 (s, 1 H), 9.05-9.03 (d, 1 H), 8.70 (s, 1 H), 8.45-8.43 (d, 1 H), 7.85-7.82 (m, 1 H), 7.81-7.78 (m, 1 H).

5-amino-1,10-phenanthroline (5-NH_2-phen). 1.960 g of **5-NO_2-phen** (8.7 mmol) were dissolved in 40 mL EtOH under Ar and then 0.5 g Pd/C (10%) catalyst was added. The reaction mixture was stirred for 30 min and 10 mL of $H_2N{\cdot}NH_2{\cdot}H_2O$ (26.7 mmol) were added dropwise over a period of 15 min. Then, the reaction mixture was stirred at 115 °C for 4 h. After the reaction was complete, the mixture was filtered, and the yellow filtrate was concentrated to 10 mL under reduced pressure. Then, the precipitate was filtered and dried under vacuum for 4 h. **5-NH_2-phen** was obtained as a yellow solid. Yield 0.75 g, (37.5 %). Anal. Calcd (%) for $C_{12}H_9N_3$: C, 73.83; H, 4.65; N, 21.52. Found (%): C, 73.02; H, 4.27; N, 20.93. FTIR (KBr, cm^{-1}): 3416 (w), 3320 (m), 3217 (m), 1634 (s), 1610 (s), 1593 (s), 1562 (w), 1505 (w), 1488 (s), 1455 (m), 1428 (s), 1406 (s), 1335 (w), 1303 (w), 1218 (w), 1128 (w), 1107 (w), 1165 (w), 1134 (w), 885 (m), 841 (s), 826 (s), 812 (m), 739 (s), 711 (w). ^1H NMR (500 MHz, $CDCl_3$): δ (ppm) 9.22 (s, 1 H), 8.96 (s, 1 H), 8.31-8.29 (d, 1 H), 8.02-8.00 (d, 1 H), 7.68 (s, 1 H), 7.52 (s, 1 H), 6.97 (s, 1 H), 3.49 (s, 2 H). ESI^+ HRMS calcd (*m*/*z*) for $C_{12}H_9N_3$ ($[M+H]^+$): 196.0796. Found (*m*/*z*): 196.0869.

[Co(5-NH_2-phen)(pymt)$_2$]PF_6 (Co (III) complex 1). $CoCl_2{\cdot}6H_2O$ (0.120 g, 0.5 mmol) was dissolved in 15 mL of MeOH and then pymtH (1 mmol) and MeONa (0.75 mmol) were added slowly. After 30 min, **5-NH_2-phen** (0.5 mmol) was added and the resulting solution was stirred at room temperature for 1 h. Then, NH_4PF_6 (0.5 mmol) was added, and the reaction mixture was stirred at room temperature for 1 h. After filtration, the filtrate was set aside to evaporate slowly at room temperature and dark green crystals of **1** were formed over a period of 3 days. Yield: 0.090 g (29%). Anal. Calcd (%) for $CoC_{20}H_{15}N_7S_2PF_6$: C, 38.66; H, 2.43; N, 15.78. Found (%): C, 38.87; H, 2.52; N, 15.59. FTIR (KBr, cm^{-1}): 3648 (w), 3382 (w br), 3227(w), 1639 (m), 1602 (w), 1565 (s), 1545 (s), 1522 (w), 1496 (m), 1470 (m), 1432 (m), 1373 (s), 1319 (w), 1257 (m), 1226 (w), 1198 (w), 1169 (m), 1065 (w), 1019 (w), 835 (s br), 798 (m), 755 (m), 718 (m), 671 (m), 556 (s). ESI^+ HRMS calcd (*m*/*z*) for $CoC_{20}H_{15}N_7S_2$ ($[M–PF_6]^+$): 476.0162. Found (*m*/*z*): 476.0234. ^1H NMR (500 MHz, CD_3CN): δ (ppm) 8.82-8.80 (d, 1 H), 8.76-8.74 (t, 1 H), 8.65-8.64 (d, 1 H), 8.62-8.61 (d, 1 H), 8.40-8.38 (d, 1 H), 8.10-8.09 (d, 1 H), 7.89-7.88 (d, 1 H), 7.87-7.86 (d, 1 H), 7.70-7.69 (t, 1 H), 7.67-7.66 (t, 1 H), 7.19-7.17 (m, 3 H), 5.68 (s, 2 H). UV-Vis (DMSO), λ_{max}/nm ($\varepsilon/M^{-1}cm^{-1}$): 296 (21700), 350 (10100), 455 (1680), 587 (150).

Exfoliated 2H-MoS_2. Bulk MoS_2 (200 mg) was mixed with 15 mL of HSO_3Cl mixture was subjected to bath ultrasonication for 8 h daily, in 30 min intervals, followed by overnight stirring (at ambient temperature), for a total of one week. Subsequently, the superacid was quenched with dropwise addition of distilled water with the mixture cooled in an ice bath, while stirring. The mixture was then filtered under vacuum through a PTFE membrane (47 mm diameter, 0.2 μm pore size) and was extensively washed until the pH of the filtrate is ~ 6.5-7. The collected residue was dispersed in 200 mL of NMP (~1 mg mL^{-1}) and subjected to probe ultrasonication for a total of 1.5 hrs. To maintain the sonication efficiency and rule out undesired high temperature issues, the sample was constantly kept in an ice bath. The dispersion was then transferred to a volumetric cylinder and allowed to settle overnight at room temperature. Finally, the upper 2/3 of supernatant volume were collected, filtered through PTFE membrane and washed three times with DMF and twice with EtOH. The solid residue was dispersed in EtOH, transferred to a glass vial and the solvent was evaporated under N_2 stream. Subsequently it was dried under high vacuum to afford 45 mg of exfoliated MoS_2 as lead grey powder.

Nanohybrid 2. In a 10 mL degassed 1,2-dichlorobenzene (oDCB), 10 mg of the exfoliated 2H-MoS_2 were finely dispersed using bath sonication. In 5 mL acetonitrile, complex **1** (3.6 mg, MW: 621.4, 0.0058 mmol) is dissolved, and they are mixed with the oDCB dispersion. After a brief sonication for homogenization and 10 min. degassing, isoamyl nitrite (2 μL, 0.0149 mmol, 2.6 equiv.) was quickly added and the mixture was left stirring for 20 hrs at 65 °C under N_2 atmosphere. Subsequently, the mixture was cooled to 45 °C, a two-fold volume of DMF was added and was then filtered through PTFE membrane filters (45 mm diameter, 0.2 μm pore size), washed 3 times with DMF, dispersed in EtOH and transferred to a vial where the solvent was evaporated under N_2 stream and overnight stay in static vacuum.

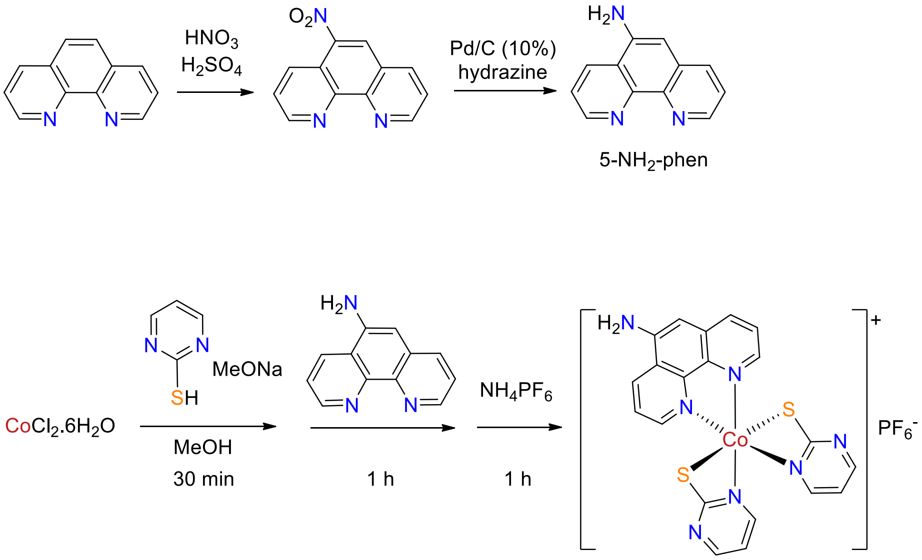

[Co(5-NH_2-phen)(pymt)$_2$]PF_6 (**1**)

Figure S1. Outline of the syntheses and drawings of the molecular structures of the ligand **5-NH_2-phen** and Co(III) complex **1**.

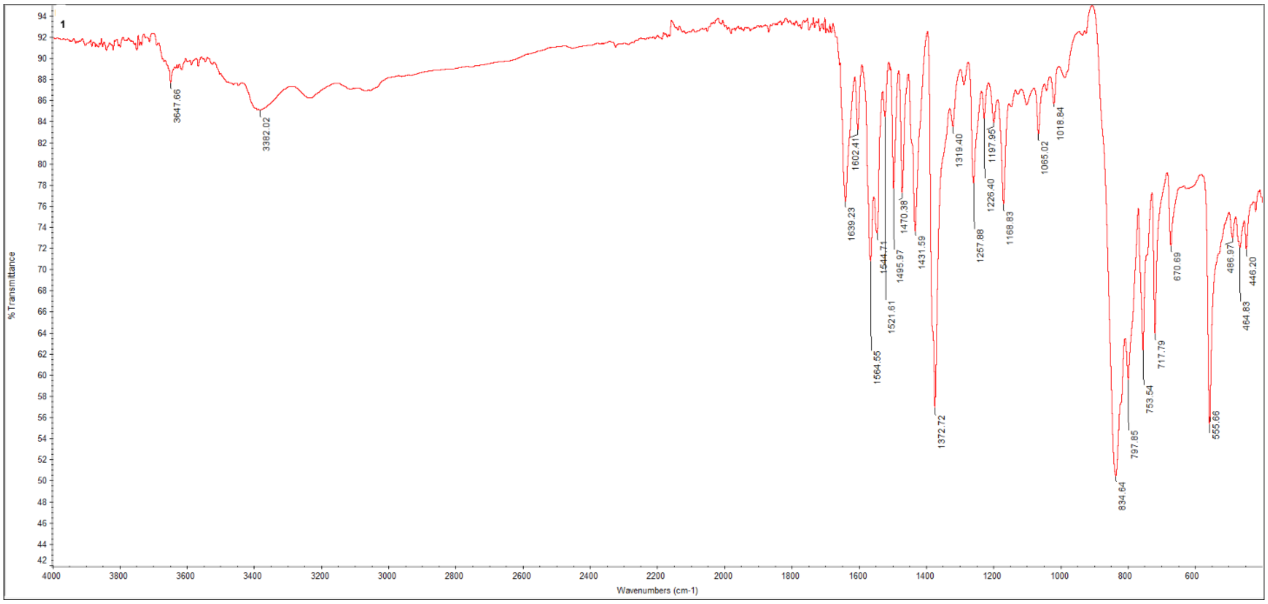

Figure S2. FT-IR spectrum of Co(III) complex **1**.

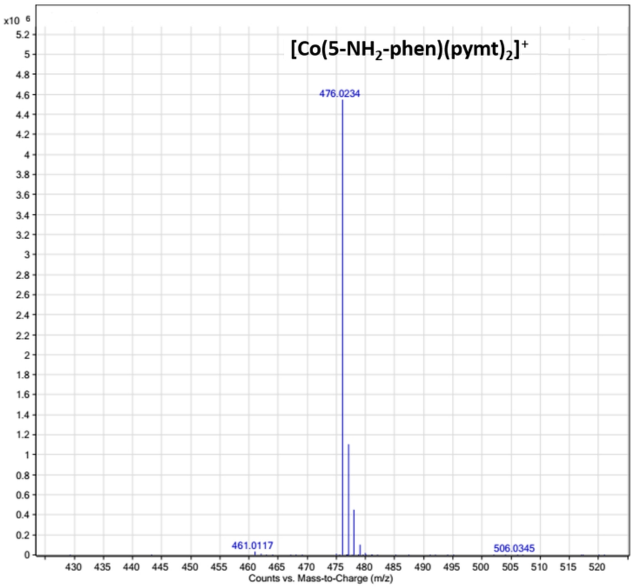

Figure S3. High-resolution ESI$^+$ mass spectrum of Co(III) complex **1**, showing a major peak at m/z = 476.0234 that corresponds to the cationic complex [Co(5-NH$_2$-phen)(pymt)$_2$]$^+$.

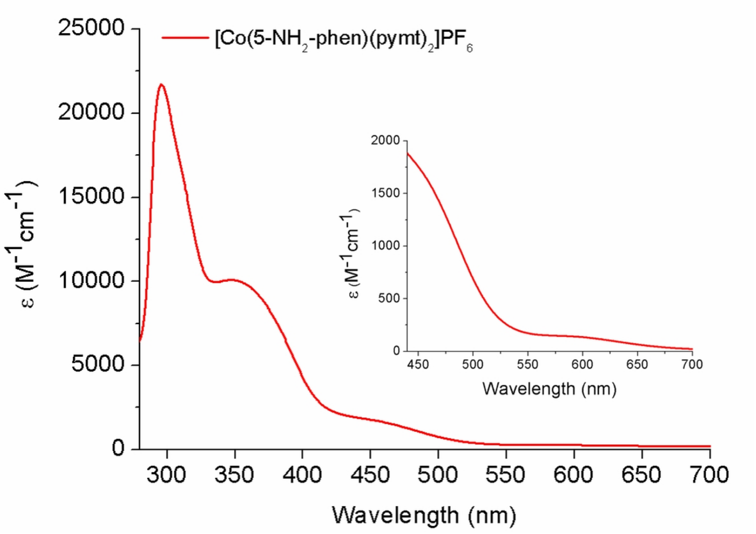

Figure S4. UV-Vis electronic absorption spectrum of Co(III) complex **1** in DMSO (1×10^{-4} M). The lower energy region of the spectrum of the complex in DMSO (1×10^{-3} M) is given at the inset.

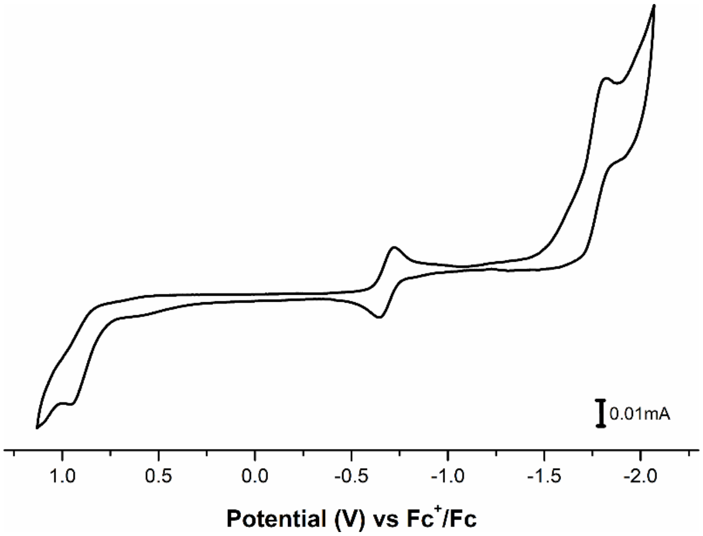

Figure S5. Cyclic voltammogram of Co(III) complex **1** in CH_3CN (10 mL, 1 mM, 0.1 M Bu_4NBF_4 as electrolyte and scan rate 0.1 V s^{-1}).

Table S1. Oxidation and reduction potentials of Co(III) complex **1** in CH_3CN (10 mL, 1 mM, 0.1 M Bu_4NBF_4 as electrolyte and scan rate 0.1 V s^{-1}).

$E_{pa}^{IV/III}$ [a]	$E_{pa}^{III/II}$ [a]	$E_{pc}^{III/II}$ [b]	$E_{1/2}^{III/II}$ [c]	$\Delta E^{III/II}$	$E_{pc}^{II/I}$
+0.94	-0.65	-0.72	-0.69	0.07	-1.81

[a, b] E_{pa} and E_{pc} are anodic and cathodic peak potentials (V), respectively. [c] $E_{1/2} = (E_{pa}+E_{pc})/2$. All potentials are referenced vs the Fc^+/Fc couple with $E_{1/2}(Fc^+/Fc) = 0.47$ V.

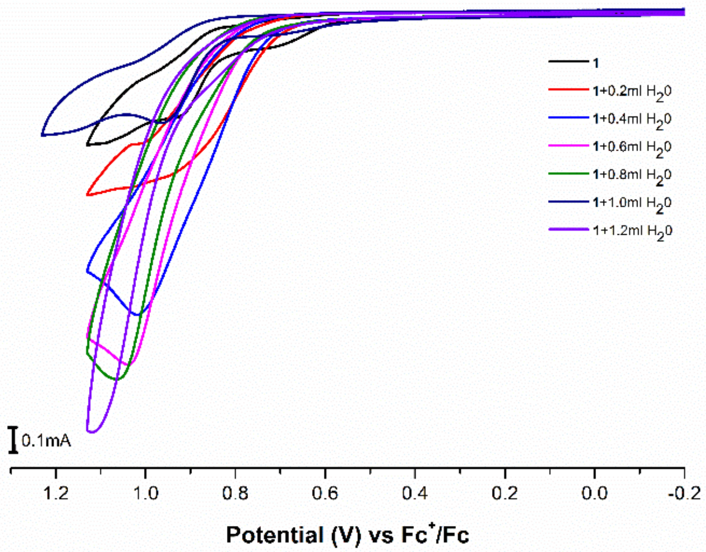

Figure S6. Cyclic voltammogram of Co(III) complex **1** in CH_3CN, showing the changes of the Co(IV)/Co(III) oxidation wave, upon addition of progressively increasing amounts of H_2O (10 mL, 1 mM, 0.1 M Bu_4NBF_4 as electrolyte and scan rate 0.1 V s^{-1}).

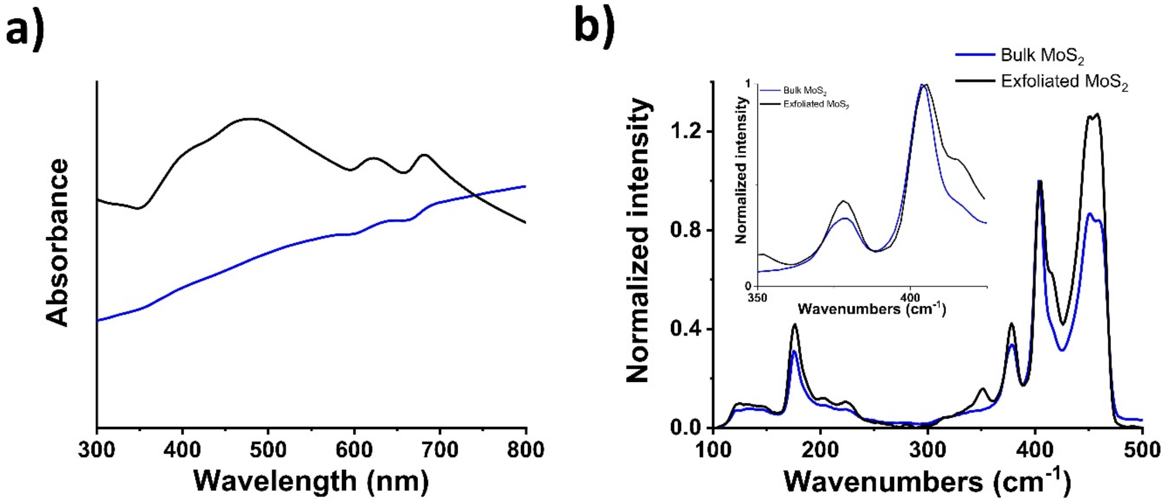

Figure S7. **a)** UV-Vis-NIR spectra in distilled H_2O, and **b)** Raman spectra, normalized at the A_{1g} mode (402 cm^{-1}) of bulk MoS_2 (blue) and exfoliated 2H-MoS_2 (black).

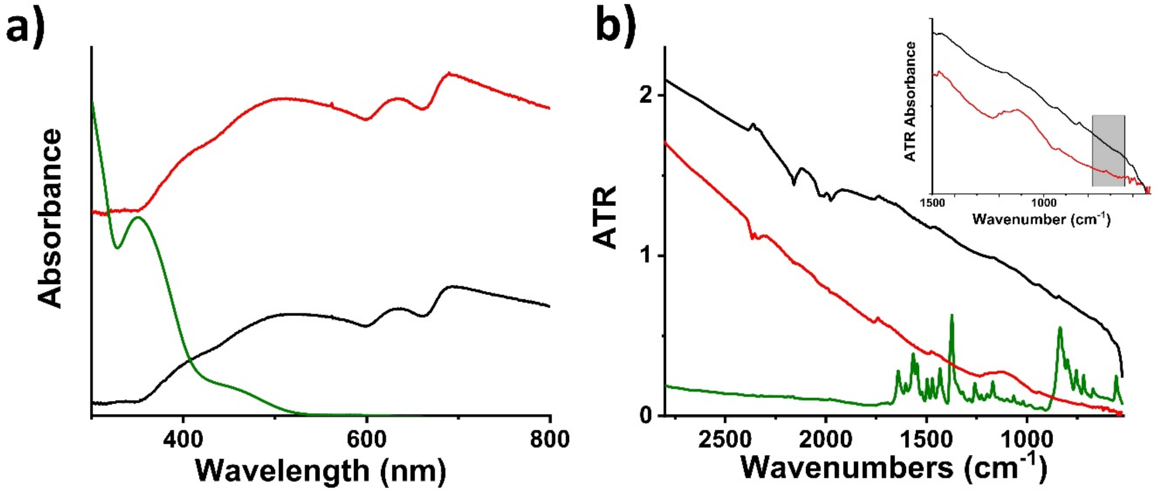

Figure S8. a) UV-Vis-NIR spectra in DMF, and **b)** FT-IR spectra, collected as ATR absorbance spectra, of exfoliated 2H-MoS_2 (black), Co(III) complex **1** (green), and nanohybrid **2** (red). Inset: blow-up image of low wavenumber area.

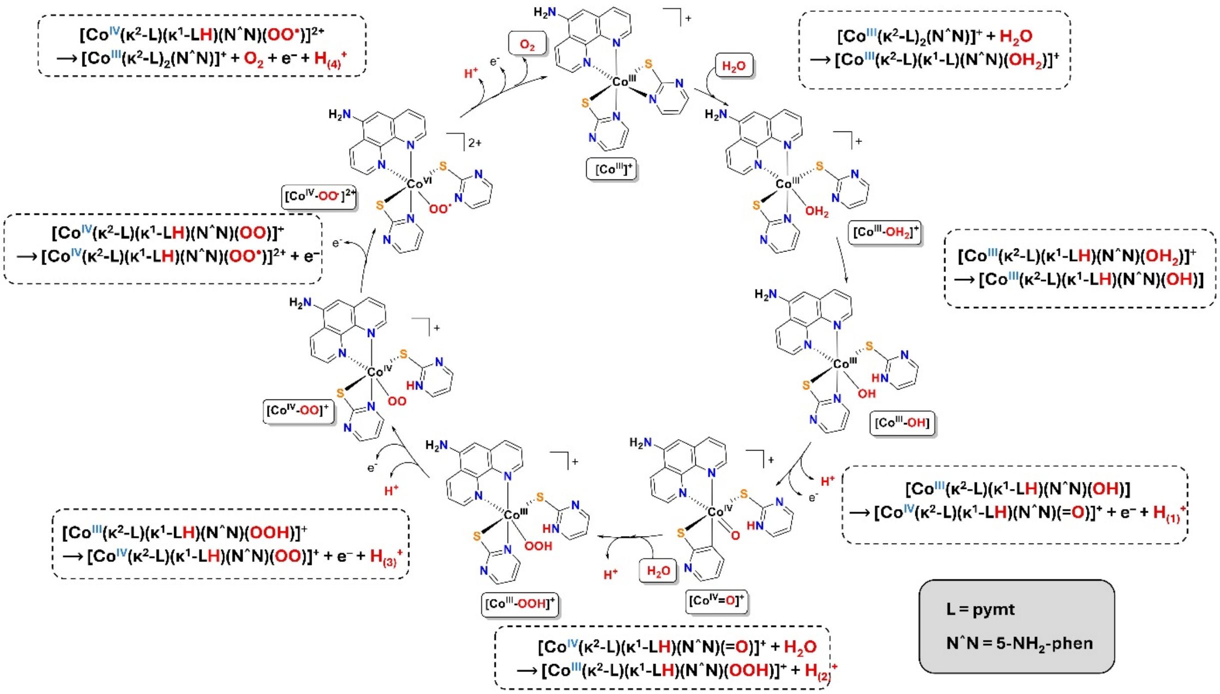

Figure S9. Schematic illustration of the proposed mechanism with equations for the electrocatalytic oxidation of H_2O to O_2 by nanohybrid **2**.